MIT Libraries | DSpace@MIT

MIT Open Access Articles

Nanometer-level alignment using interferometric-spatial-phase-imaging (ISPI) during silicon nanowire growth

Massachusetts Institute of Technology

Nanometer-level alignment using interferometric-spatial-phase-imaging (ISPI) during silicon nanowire growth

Pornsak Srisungsitthisunti[a], Euclid E. Moon[b], Chookiat Tansarawiput[c], Huaichen Zhang[a], Minghao Qi[c], Xianfan Xu*[a]

[a]School of Mechanical Engineering, Birck Nanotechnology Center, Purdue University, West Lafayette, Indiana 47907;
[b]NanoStructures Laboratory, Research Laboratory of Electronics, Massachusetts Institute of Technology, Cambridge, Massachusetts 02139;
[c]School of Electrical Engineering, Birck Nanotechnology Center, Purdue University, West Lafayette, Indiana 47907

ABSTRACT

We describe a method of detecting nanometer-level gap and tip/tilt alignment between a focusing zone plate mask and a silicon substrate using interferometric-spatial-phase-imaging (ISPI). The zone plate mask is used to generate sub-micrometer focused light spot to induce silicon nanowire growth in a CVD process. ISPI makes use of diffracting fringes from gratings and checkerboards fabricated on the mask to determine the correct gapping distance for the focusing zone plates. The method is capable of detecting alignment inside a gas-flow chamber with variable pressure.

Keywords: nanometer alignment, interferometry

1. INTRODUCTION

Nanometer-level alignment is essential to enable several nano-fabrication techniques such as nanolithography and imprint lithography. The mask and substrate alignment must be achieved with nanometer-level accuracy in all six degrees of freedom (X, Y, Z, yaw, pitch, and roll). Several alignment methods rely on interference of light to detect sub-wavelength alignment [1-5]. A white-light scanning interferometer measures the air gap thickness acting as a modulator from the source and eliminates any chromatic dispersion issue [5]. However, this method requires scanning to calculate absolute gap. Interestingly, a nanogap can be measured using surface plasmon resonance, but material and gap range are very limited [6]. Interferometric-spatial-phase-imaging (ISPI) utilizes specialized grating and checkerboard patterns on the mask and substrate to produce interference fringes. Alignment is determined from Fourier-based phase-difference analysis. ISPI has been proved to achieve alignment better than 1 nm sensitivity in gap and lateral alignments [1-4]. Advantages of the ISPI method include non-scanning scheme, high signal-to-noise ratio, and fluctuation tolerance. Since our substrate does not contain pre-existing features, lateral alignments are unnecessary and only gap alignments are discussed.

In this paper, we investigate the use of ISPI alignment scheme for silicon nanowires growth with laser direct writing. The silicon nanowires are grown inside a chemical vapor deposition (CVD) chamber, supplied by a mixture of silane ($SiH4$) and nitrogen. A substrate (Si or SiO2) was selectively heated and scanned with laser pulses to induce nanoscale lines of Si deposit on the substrate. Laser beam was focused by a Fresnel zone plates fabricated on the mask to produce a diffraction-limit spot of ~250nm on the substrate. Details of the growth processes and materials are presented elsewhere [7]. A feedback control software was implemented to maintain the constant gap during the growth. With the ISPI alignment and the feedback control, we successfully produced uniform laser direct writing lines with 250nm linewidth on the substrate.

*xxu@ecn.purdue.edu

2. EXPERIMENTAL SETUP

The laser direct writing of nanowires setup consists of three main parts: the laser source, the vacuum chamber, and the ISPI scope. A pulsed frequency-doubled Ti:Sapphire laser (400nm wavelength) with 50 femtosecond pulsewidth is directed inside the vacuum chamber through a quartz window and focused on a substrate. The smallest focal spot of ~250 nm is achieved by a Frenel zone plate (NA 0.95) fabricated on the mask. The vacuum chamber is connected to a multi-gas flow panel and a mechanical pump. Inside the chamber, the substrate is clamped on a 5-axis piezo stage (X, Y, Z, θx, θy) with 0.4 nm translational and 6 nrad angular resolutions. Above the substrate, the mask is held by a custom kinematic mount and a linear height stage (θx, θy, Z). All the positioning of the mask and the substrate are computer controlled. The mask contains zone plates having a focal length of 50 μm, so the substrate must be held at 50 μm below the mask. The gas flows through a nozzle pointing toward the substrate. The ISPI scope is mounted on a custom breadboard outside the chamber.
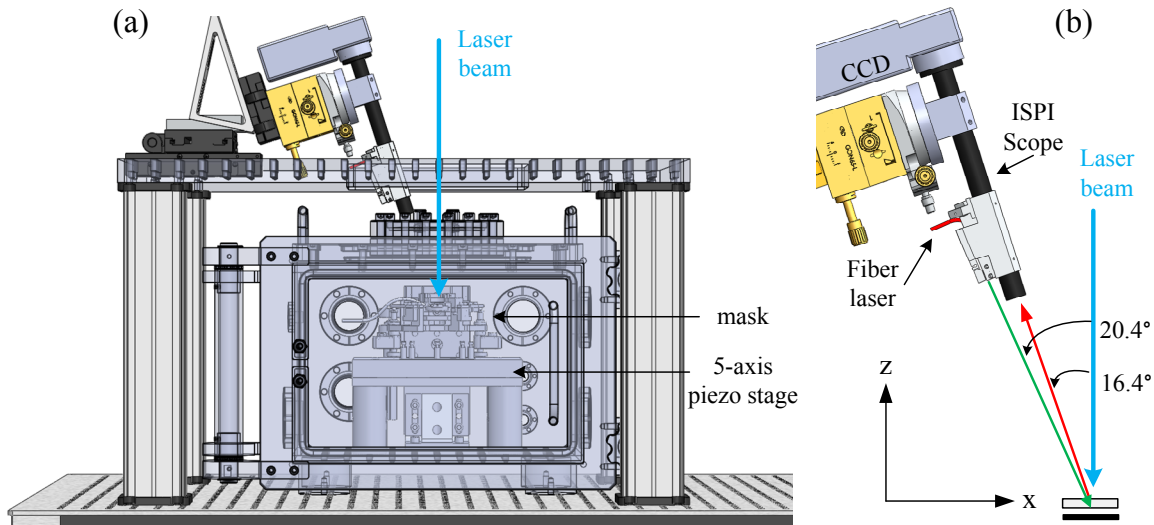

Figure 1. Experimental setup of ISPI alignment above a vacuum chamber. The ISPI scope is fixed with 6-axis stage control, viewing the mask and the substrate alignments from off-axis angle through the top quartz window.

Figure 1(a) shows a model of the experimental setup. The ISPI scope (12x magnification lens) with a long working distance (110 mm) is oriented to view through a top quartz window of the chamber. The mask-substrate alignments are observed via the ISPI scope at a specific incident angle, as shown in Fig. 1(b). A fiber laser with a wavelength of 630 nm is attached to the ISPI scope, where the scope is fixed to a 6-axis control stage. The angle between the laser beam and the scope is adjustable and set to ~4 degree. Incident angle, symmetric angle, and rotation of the ISPI scope must be adjusted correctly for an accurate ISPI detection.

To obtain the ISPI signal, the laser beam is incident on the mask and diffracted through the mask and substrate before reflected back to the ISPI scope. Chirped and unchirped gratings and checkerboards patterns on the mask are used to obtain different types of alignment signal. The laser beam incident angle is critical to ensure that the mask-substrate signal is calculated correctly. The ISPI fringe signal is captured with a CCD and analyzed with Labview software. The ISPI scheme produces high signal-to-noise ratio due to off-axis viewing angle, eliminating directly-reflected background. Moreover, the alignment signal is insensitive to fluctuations in wavelength, intensity, or change of the refractive index in the beam path. ISPI gap detections use special grating pattern on the mask and do not require any pattern on the substrate. Therefore, any blank smooth reflective substrate is detectable by the ISPI gapping scheme.

Mask containing ISPI patterns and Fresnel zone plates were fabricated on an optically flat quartz by the following steps. First, the quartz is cleaned and evaporated with a 140-nm thick of indium tin oxide (ITO) as a transparent conducting layer for e-beam lithography. A 470-nm thick of hydrogen silsesquioxane (HSQ) is spun on top of ITO and ISPI and

zone plates are patterned with e-beam lithography. After HSQ developing, the quartz is baked at 500°C to harden the HSQ ;the final thickness should be 457 nm (π phase shift for 400 nm illumination). The SEM images of zone plate and ISPI pattern are shown in Fig. 2. The ISPI pattern contains several grating and checkerboard patterns for different functions such as incident-angle-checking, coarse gapping, and fine gapping.
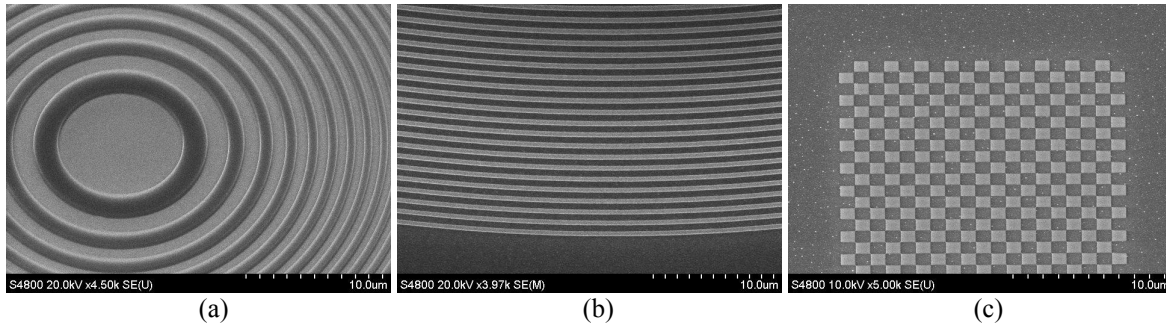

| (a) | (b) | (c) |

Figure 2. SEM images of a mask containing (a) zone plate with high quality at (b) the outer rings, and
(c) a small section of the ISPI mark containing a checkerboard pattern.

3.   COARSE AND FINE GAP DETECTIONS

Initial alignments are required before any gap detection is calculated. The incident angle must be known to accurately calculate a coarse gap. The ISPI scope angle is aligned by either using a digital level or an incident-angle-checking pattern on the mask. The incident-angle-checking use chirped checkerboard pattern to diffracted beam symmetrically at a specific incident angle. The ISPI is designed to operate close to the Littrow angle for a higher signal-to-noise ratio. Similarly, the side-to-side angle (symmetric across the XZ plane) of the incident beam is checked with another incident-angle-checking pattern.

The coarse gap detection is a convenient way to level the mask and avoid collision. The working range is >30 μm gap with detectivity <1 μm. A bar grating with 1 μm period is used as shown in Fig. 3(a). The beam is incident to the bar grating, producing one imaged spot from the direct back diffraction, and the other spot from the substrate reflection of the forward diffraction. The absolute gap is calculated from the separation of the two bar images with a known incident angle. The coarse gapping can be understood directly since the smaller gap will produce a smaller separation between the two bar images resulted from a back-diffracted beam and a diffracted-reflected beam. This is shown in Fig. 3(b). To level the mask to the substrate, coarse gaps at three different locations are measured and adjusted simultaneously. In practice, mask leveling of 0.5 mrad or better is achieved by this method. If the gap is decreased below 30 μm, the two bar images overlap and interfere.
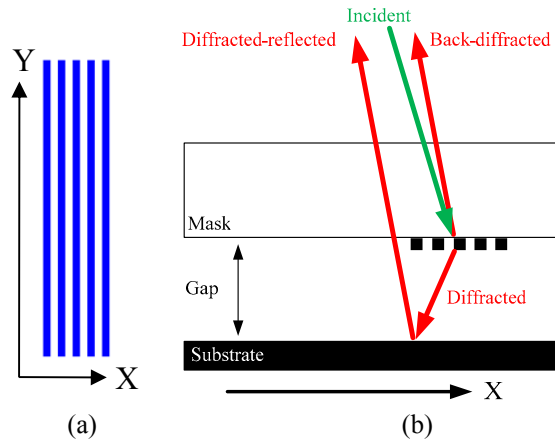

| (a) | (b) |

Figure 3. (a) Coarse gap pattern and (b) schematic of the incident beam is back-diffracted
and diffracted-reflected to generate two separated imaged back to the ISPI scope.

Fig. 4(a) illustrates the fine gap detection utilizes a two dimensional (2D) checkerboard grating, where the X periodicity is uniform and the Y periodicity is chirped. The beam is incident along the X axis and the uniform X grating is designed to diffract back the beam to the scope. The chirped Y grating produces gap-dependent interference fringes in the image. The use of the interference fringes of chirped grating to determine an absolute gap is referred to as transverse chirp gapping (TCG).

In order to understand how the TCG scheme works, we consider X diffraction and Y diffraction separately. The X periodicity is designed to be 1 μm and the wavelength of the fiber laser is 630 nm, resulting in a Littrow angle of $\theta = \sin^{-1}(\lambda/2\Lambda) = 18.4$ degree. Given that the laser beam and the scope is 4 degree difference, the incident and the first-order diffracted angle should be 16.4 and 20.4 degree, respectively. Therefore, the ISPI scope only sees the signal from the first order diffraction of the primary and secondary beams as shown in Fig. 4(b). This is also the working principle for the coarse gap of the bar grating.

On the other hand, since the periodicity in the Y is chirped, the angle of the transmitted-diffracted beams will vary along the Y direction and so will the mask-substrate-mask path length. Therefore, the chirped grating diffracts beams in a sweep of angles along the Y direction. Subsequently, the beams reflect from the substrate, and rediffract from the mask at some distance from where they originally diffracted. Interference fringes from the rediffracting beams returns toward an ISPI scope due to X grating. The fringes are parallel to the X axis and interference fringes are sensitive in both position and frequency as the gap varies. Two TCG patterns with their chirps in opposite directions result in fringes that counterpropagate when the gap is changed. Their relative phase encodes position which eliminates ambiguity when used with the corresponding fringe frequency.
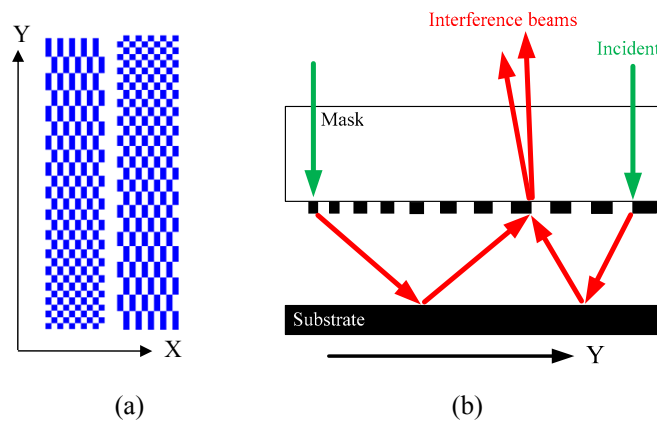

(a)   (b)

Figure 4. (a) Fine gap pattern and (b) schematic of diffracted beam in the YZ plane, showing an example of two incident beam that diffract, reflect, and rediffract, producing contractive interference.

TCG fringes vary in frequency, phase, and intensity, as gap is changed. The fringe frequency depends on the gap due to the interaction distance along the chirp. As the gap decreases, interfering beams travel a smaller transverse distance, resulting in a small difference in grating periods; hence larger distance between constructive interference. Conversely, the interaction distance increases with larger gap, causing more disparate spatial frequencies to interact, which results in higher fringe frequency. The rate of change in fringe frequency can be determined experimentally and different fringe sensitivities as a function of gap is designed based on the chirp rate.

The sensitivity of the fine gap detection is determined from a measurement of the relative phase difference between two opposite TCG fringes. From calibration, phase change of 2π corresponds to a 200 nm gap change. A change of 30 nm gap results in 53 degree phase difference is detectable by eyes. However, the ISPI phase algorithm is capable of detecting < 1/2000 of a fringe cycle, which is 200nm/2000 = 0.1 nm gap sensitivity.

4. RESULTS

Gap detection by the ISPI method was tested for its accuracy and repeatability. The performance of the ISPI gap reading can be verified by using a known gap or a known gap displacement. The most straightforward test is moving the piezo stage a certain distance and compare with the change of the ISPI reading. The accuracy of the gap change was tested in a displacement range of 10-100 μm. The average gap error was smaller than 0.5 μm for several repeated displacements. The error of the gap reading was due to a small brightness fluctuation of the two bar images at different gaps, causing misinterpreting of the actual gap. However, the repeatability was better than 50 nm from several readings. The high repeatability significantly helps produce uniform lines during direct laser writing of nanowires. The coarse gap detection was sufficient for the zone plate focusing with a depth of focus of 1 μm. The coarse gap detection showed that our system has ~30 nm noise level. Figure 5(a) shows the ISPI signals from the coarse and fine gap detections at different gaps. For coarse gap, smaller separation between the two bars indicates a smaller gap.

The fine gap method relies on the counterpropagating vertical fringes and the phase difference between the two opposite TCG was calculated by comparing with the simulated fringes at different gap. The experiment showed that as the gap decreases, the vertical fringe periodicity increase as shown in Fig 5(b). The fine gap algorithm is highly sensitive to signal fluctuation. However, our system was subjected to vibration that disturbed the fine gap detection to give a stable reading.
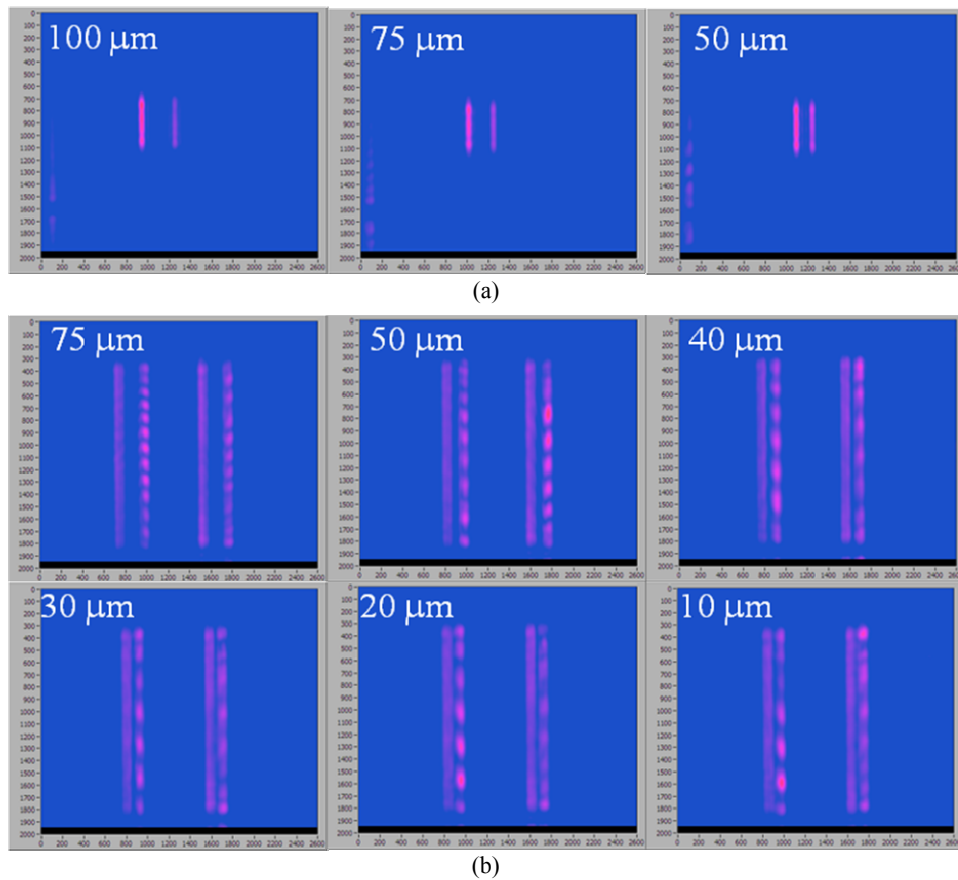

(a)

(b)

Figure 5. Experimental demonstration of (a) ISPI coarse gap detection and
(b) fine gap detection at different gaps.

During the laser direct nanowire growth, several disturbances in the system can easily cause misalignments such as the followings. The CVD chamber is directly connected to the mechanical pump, which generates vibration. We often turned off the pump during the growth to avoid vibration. Thermal expansion due to cumulative laser exposure and/or external heater, which was required for some growth processes, induced significant change in mask-substrate gap. In

addition, piezo stage was drifted small amount over time, due to gas flow and/or other factors. If the mask and the substrate are nonparallel, lateral scanning of the substrate changes the gap. In order to obtain a diffraction-limit resolution, the substrate must be positioned exactly at the focal length of the zone plate and parallel to the zone plate during laser scanning. Therefore, the feedback control is necessary to constantly compensate for correcting any changes in alignments.

By using the ISPI reading, the piezo stage was programmed to correct any gap change in real time. Since the response time of the stage is as fast as 5 ms, a range of gap correction and a delay time were set properly to avoid rapid vibration due to non-stop feedback correcting. As a result, the feedback control was effective against slow misalignment, such as stage drift, tilt scanning, and heat expansion. Figure 6 compares the use of feedback control in our system; the mask-substrate gap drifted ~0.5 µm over 10 minutes, but with the feedback control it stays within 0.1 µm. Moreover, we demonstrated a burn test by using a Fresnel zone plate focused laser at 50 µm focal length on a silicon substrate. The ISPI and feedback control successfully produce uniform Purdue logos with linewidth smaller than 300 nm, as shown in Fig. 7.

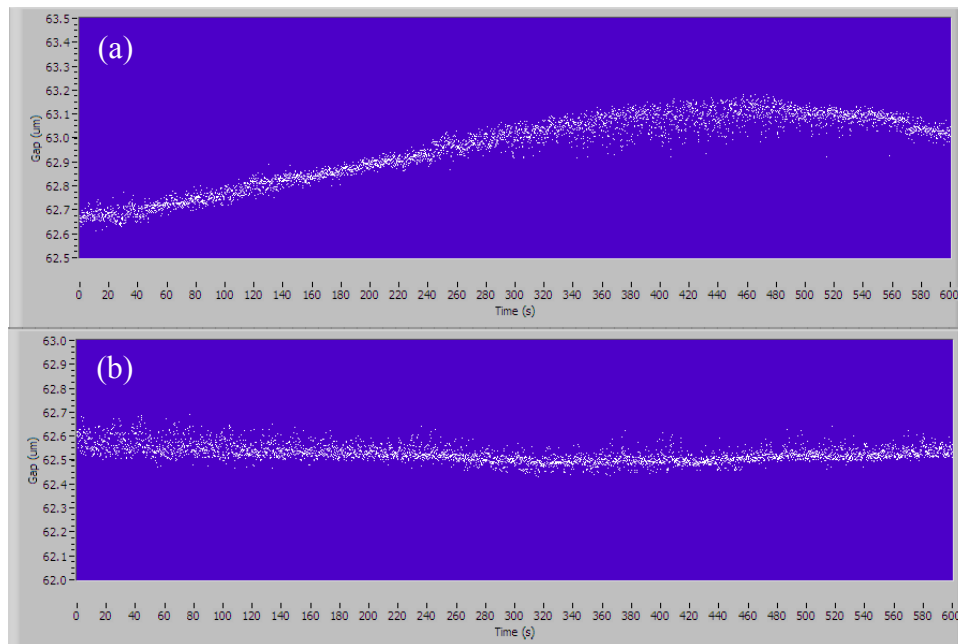Figure 6. ISPI gap monitoring over 10 minutes duration with (a) no feedback control and
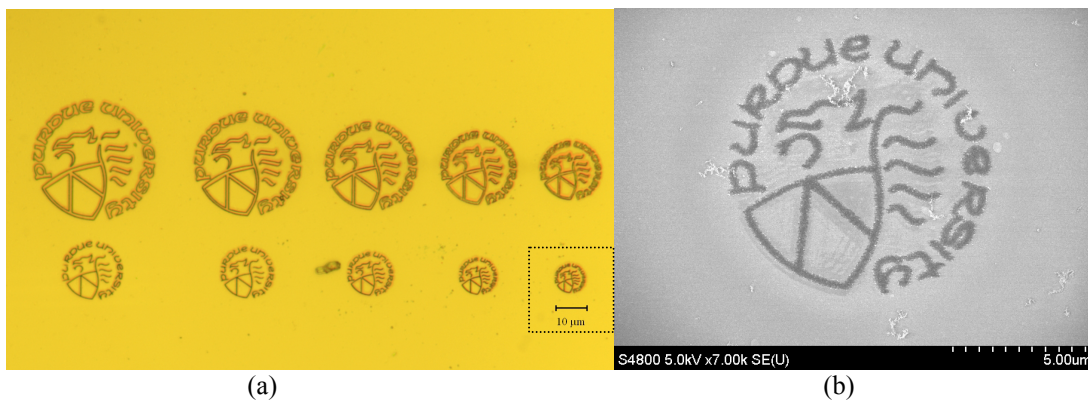(b) with feedback gap correction set at 62.5 µm.

(a) (b)

Figure 7. (a) Microscope image of laser direct written Purdue logos on a silicon substrate
(b) SEM image of the selected logo

5. DISCUSSIONS AND CONCLUSION

We have demonstrated the use of ISPI gap detection in a CVD system. The purpose of the gap detection is to level the substrate to the mask and position the substrate at the focus spot of a zone plate. Coarse gapping scheme showed sensitivity better than 30 nm. Using the coarse gapping, the gap can be positioned within 0.5 μm accuracy and 50 nm repeatability. The coarse gapping is sufficient at this level to create 250 nm lines with Fresnel zone plate. The feedback control was integrated with the coarse gapping signal to maintain the desired gap during the nanowires growth. The feedback control effectively eliminated gap change due to stage drift and unparallel scanning, maintaining the gap within 100 nm. Under CVD chamber conditions, we successfully controlled the gap alignment in nanometer-level and produced uniform 250-nm-width laser direct writing lines.

REFERENCES

[1] Moon, E. E., Chen, L., Everett, P. N., Mondol, M. K., and Smith, H. I. "Interferometric-spatial-phase imaging for six-axis mask control," *J. Vac. Sci. Technol. B*, **21**, 3112-3115 (2003).

[2] Moon, E. E., Mondol, M. K., Everett, P. N., and Smith, H. I. "Dynamic alignment control for fluid-immersion lithographies using interferometric-spatial-phase imaging," *J. Vac. Sci. Technol. B*, **23**(6), 2607-2610 (2005).

[3] Moon, E. E., and Smith, H. I. "Nanometer-precision pattern registration for scanning probe lithographies using interferometric-spatial-phase imaging," J. Vac. Sci. Technol. B, 24(6), 3083-3087 (2006).

[4] Menon, R., Moon, E. E., Mondol, M. K., Castano, F. J., and Smith, H. I. "Scanning-spatial-phase alignment for zone-plate-array lithography," *J. Vac. Sci. Technol B*, **22**(6), 3382-3385 (2004).

[5] Xu, Z., Shilpiekandula, V., Youcef-toumi, K., and Yoon S. F. "White-light scanning interferometer for absolute nano-scale gap thickness measurement," *Optics Express*, **17**, 17, 15104 (2009).

[6] Wu, P. T., Wu M. C., and Wu, C. M. "A nanogap measuring method beyond optical diffraction limit," *J. Appl. Phys.* **102**, 123111 (2007).

[7] Mitchell, I. J., Park, J. S., Watson, A. C., Srisungsitthisunti, P., Tansarawiput, C., Qi, M., Stach, A. E., Yang, C., Xu, X., "Femtosecond laser direct writing of nanoscale silicon lines," Proc. SPIE 7764-13 (2010).